Spring 5-2022

Toward long non-coding RNA detection using DNA nanoswitches

Ché-Doni Platt

Toward Long Non-Coding RNA (lncRNA) Detection Using DNA Nanoswitches

An honors thesis presented to the
Department of Biological Sciences,
University at Albany, State University of New York
in partial fulfillment of the requirements
for graduation with Honors in Biochemistry and Molecular Biology
and
graduation from The Honors College

Ché-Doni Platt

Research Mentor: Arun Richard Chandrasekaran, Ph.D.
Research Advisor: Ken Halvorsen, Ph.D.
Second Reader: Gabriele Fuchs, Ph.D.

May 2022

Abstract

Long non-coding RNAs (lncRNAs) are transcripts that are over 200 nucleotides and do not encode proteins. LncRNAs are involved in a wide spectrum of biological processes ranging from cell proliferation, apoptosis, and nutrient sensing to cell differentiation. Further, lncRNAs have been reported to play an important role in a wide range of pathophysiological processes and are linked to diseases such as cancer. Thus, lncRNAs are becoming increasingly important as biomarkers to study biological and disease processes. In our work, we develop a DNA nanoswitch-based assay for detecting long RNAs. The DNA nanoswitch is a reconfigurable device that undergoes a conformational change from a linear "off" state to a looped "on" state upon interaction with the target molecule. The two states can be easily identified on an agarose gel. Using in vitro transcribed RNA controls, we optimize the assay for detecting different lengths of target RNAs, validate the sensitivity and specificity of the assay, and detection of target RNA in the presence of total RNA extract. Our work aims to create a lncRNA detection assay that will be useful in the early treatment of diseases and in screening potential biomarkers (for example, in Duchenne Muscular Dystrophy). The DNA nanoswitch-based assay is low-cost, highly sensitive and specific, and easily adaptable in any laboratory for detecting various biomarkers.

Keywords: *Long non-coding RNAs*, *DNA nanoswitches*, *disease biomarkers*

Acknowledgments

In loving memory of Nicola Lee-Platt PhD
(Mommy)
1974-2015
"Thanks for the grit and giving me your whole self"

To my Aunty Joan, I love you and I appreciate your sacrifice.

The first of many papers I am honored to put my name on as the primary author. I am grateful to God and my entire family for allowing me to exercise this opportunity to fully be present and healthy in my research pursuits, to my PI, Ken for accepting my presence in the lab wholeheartedly, engaging with me in conversation, and giving profound advice and insight into his intellect. I would also like to extend immense gratitude to my mentor, Arun. Thank you for stretching my mind, my vocabulary and enforcing time constraints on me. I may laugh at it all in the moment, but your mentorship has had a lasting impact on me and helped in the cultivation of the professional I know I will be someday. I would especially like to thank you for reintroducing the phrase "Don't worry, be happy." You have a knack for recognizing when to demand more and when to rest easy. I hope to cultivate that awareness. To Jibin, thank you for being a second mentor, though many times a silent one. Your work ethic, thoughts, and conversations have expanded my knowledge and appreciation for single-molecule techniques and physics in general. To Andrew, thank you for making extra gels in the morning, challenging my thoughts on the experiments I was performing, and giving me so much insight into baking. We won best taste at RNA Day because you made my gel cake come to life. To Javi, I enjoyed how easy it was to approach you with any questions I had and mistakes I made. You made me feel comfortable in my innocence about the lab and I surely grew from it. I would also like to thank you for being my football watching lab partner. It was a lot more homily watching Champions League matches between experiments. To Asmer, thank you for your invaluable feedback on my presentation skills and the intricate details about my approach and mannerisms. It means the world to get your feedback because you have made me a better presenter for it. Now, for the 'Peru, para' crew that took on San Francisco. Kevin, thanks for being my rock in and outside of lab. We started this lab journey together and we have achieved so much – grown so much. You have helped me practice presentations, with posters, with award applications, make figures, take pictures, make buffer – the whole bit. I am extremely happy we both ended up in Halvorsen Lab. You push me to be better. To Cheyenne, my roommate and hopefully future travel buddy, thank you for your calmness, your presence on our trip, in lab, and in all the things we both do on campus, you have been a force to help ground my overthinking at times. To Nate, your energy is unmatched. It is a joy to be around you and to have your senior experience in the lab as an inspiration. To Akul, you are a G, when you joined the lab, it was like my happy meter broke. Your hairstyles kept me guessing and your journal club presentations increased my appreciation for science. Arlin, you make some of the nicest figures, have the most bomb hair and you work so quickly and efficiently, I look to you for inspiration. Lifeng, your presentation at a COVID-19 panel inspired me to send my email to Ken, thank you for that. Thank you, Dr. Fuchs, for making me love molecular biology and for your invaluable feedback as my second reader. This work has stretched me for the better, putting into practice a lot of the techniques I learned about in my biochemistry and molecular biology classes. I have grown in this position, and I will be forever grateful for this opportunity.

List of Figures

Table of Contents

Introduction

Biomarkers and their importance

According to the Food and Drug Administration (FDA), a biomarker is a "defined characteristic that is measured as an indicator of normal biological processes, pathogenic processes, or responses to an exposure or intervention, including therapeutic interventions".[1] The determination of various biomarkers is important to understand the pathophysiology of organisms. Their realization will lead to the development of diagnostic testing and possible therapeutics for medical conditions. Biomarkers can be grouped as histologic, radiographic, physiologic, or molecular.[1] Histological biomarkers are represented as biochemical/molecular alterations of cells, tissues, or fluid samples at various stages.[2] For example, histological biomarkers may be representatives of the stages of tumors for cancers. Radiographic biomarkers are those obtained through radio-imaging.[2] An example of this is the size of a tumor as a cancer progresses. Physiological biomarkers are measures of the body processes, such as blood pressure. Molecular biomarkers are those with biophysical properties which are measurable in a biological sample; a simple example of this is blood glucose level. Molecular biomarkers have the potential to increase the robust nature in which diagnoses are made and treatments are studied and developed. As medicine moves towards a more individualistic basis of treatment, the molecular level will become increasingly important to determining diseased states or conditions early on in development as well as the potential treatment options for a patient. For instance, miRNAs have been shown to be differentially expressed in the blood of cancer patients and could serve as a molecular indicator of the diseased state.[3]

lncRNAs as biological markers

LncRNAs are RNA transcripts exceeding 200 nts in length that do not code for proteins.[4,5] Their expression in mammalian tissue has been studied increasingly over recent years.[6] Of the lncRNAs discovered, many are regulators of gene expression and modulators of epigenetic states.[7,8] LncRNAs are involved in a variety of biological pathways inclusive of cancer pathways,[9,10] hypertension,[11] cardiometabolic diseases,[12] stroke,[13] and epigenetic splicing events.[14]

As more information emerges surrounding the world of lncRNAs, the quantification of known lncRNAs has been somewhat lacking.[15,16] Previous analysis of lncRNA expression found that lncRNAs may be present in low levels in bulk tissue samples but in higher levels in individual cells.[17] The difficulty in detection is notable because identification of specific lncRNAs may be varied as the copies present per cell may be few or specific to only certain cells. Further, lncRNAs may be characterized by the presence or lack of polyadenylated tails[18] which may limit quantification using popular techniques such as RNA sequencing. This may also complicate lncRNA discovery as non-coding regions possessing polyadenylated caps suggest some protein coding function or mutation in mRNA sequences.

So far, lncRNAs have been detected using microarrays, qPCR, and Next Generation Sequencing.[19] These detection methods, while showing high sensitivity and specificity, are costly, requiring expensive equipment and skilled personnel. Some of these methods also provide indirect quantification of lncRNAs increasing variation in the actual proportions in total RNA. Thus, newer, alternate methods that can provide low-cost and direct detection of lncRNAs are needed.

DNA nanotechnology-based biosensing methods

Beyond the traditional methods such as PCR, microarrays and Next Generation Sequencing, the field of DNA nanotechnology has been booming with methods to detect, sense and quantify various biomolecules.[20,21] In DNA nanotechnology, DNA is used as a material to construct various shapes and structures in the nanoscale.[22–24] These structures have been used in applications such as biosensing,[20] drug delivery,[25] cell modulation,[26] molecular computation,[27] and data storage.[28] DNA devices developed for biosensing include DNA-PAINT (DNA-based points accumulation for imaging in nanoscale topography) used for 3D imaging and quantifications of proteins,[29] I-Switch for pH-detection,[30] DNA polyhedra for nucleic acid detection,[31] and DNA origami-based structures for detecting antigens.[32] In our lab, we have developed DNA nanoswitches to detect several biomarkers such as microRNAs, viral RNAs, enzymes and antigens.

DNA nanoswitches – Design, operation and read out

The DNA nanoswitch is a biosensing device comprised of a linearized single stranded (ss) M13 scaffold (7249 nucleotides) made double stranded by annealing short complementary backbone oligonucleotides (Figure 1a) that are 49-60 nt each.[33–35] Two of these backbone oligos are modified to contain single stranded extensions (detectors) that are complementary to parts of the target RNA. The constructed nanoswitch is said to be in a linear "off" state. Upon binding a target nucleic acid, the nanoswitch undergoes a conformational change from the linear "off" state to a looped "on" state (Figure 1a). Binding of the target RNA to the detectors can be visualized by agarose gel electrophoresis (Figure 1b). The nanoswitches are stained using regular DNA gel stains (Gel Red in this case) providing a direct readout. As the samples run through the gel, the "on" nanoswitches run slower through the pores of the gel compared to the "off" nanoswitches (indicated by the two

bands in the experimental lane referred to as positive (+) in Figure 1b). This assay, compared to the previously discussed methods of PCR, Microarrays and Next Generation Sequencing, is quick, low cost and adaptable for bench top experimentation in most lab settings.

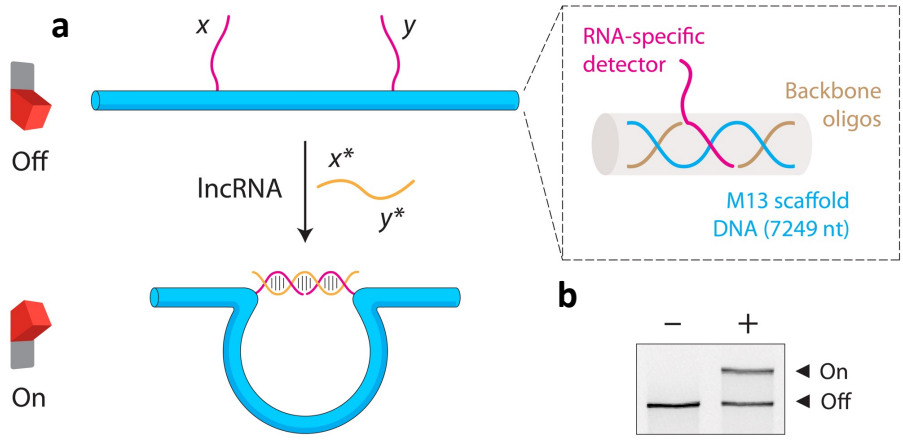

Figure 1. DNA nanoswitch design, operation and read out

(a) The DNA nanoswitch consists of a linear M13 single strand hybridized to backbone oligonucleotides two of which are modified to contain single stranded extensions (detectors). These extensions are designed to be complementary to parts of the target RNA. When both detectors base pair with the target the nanoswitch undergoes a conformational change from the linear (off) state to a looped (on) state. (b) The results of this conformational change may be visualized on an agarose gel where the "on" nanoswitches migrate differently on the gel compared to the "off" nanoswitches.

In previous work, our lab has used the DNA nanoswitches for detecting nucleic acids,[36–38] antigens,[39] and ribonucleases.[40] For nucleic acids, we have shown detection of microRNAs (miRNAs). MiRNAs are short sequences of RNA, approximately 22 nucleotides (nt) in length that do not encode proteins.[21] They are known to regulate gene expression post transcriptionally through antisense binding to messenger RNA (mRNA).[41] In our lab, we have developed a nanoswitch based assay for the detection and quantification of miRNAs specific to skeletal muscle

differentiation[38] and Alzheimer's Disease (AD)[37] using a microRNA activated conditional looping of engineered switches (miRacles) assay. Alzheimer's Disease, AD, a neurodegenerative disorder, has been studied for many years to achieve early detection and treatment options for individuals currently with and those pre-disposed to the development of AD. Further work in our lab on AD-associated miRNAs showed variable levels of specific miRNAs in total RNA isolated from different regions of the brain, showing dysregulation in healthy versus diseased samples.[37] The importance of this is profound as these miRNAs have the potential to assist in the development of non-invasive diagnostic methods for AD, therapeutic treatments and increased understanding of the disease.

In addition to our study of AD which has had chronic impacts on the aging population, our lab has also achieved rapid detection of the more acute SARS-CoV-2, a viral RNA.[36] Viral RNAs are long pieces of RNA originating from RNA viruses. These viruses invade living cells and utilize the transcriptional machinery of the host to mutate, increasing the viral RNA load. As such, viral RNAs are molecular biomarkers which may indicate the existence and progression of an infection. This is the RNA virus that caused the COVID-19 pandemic we continue to experience today. The detection of SARS-CoV-2 RNA has been achieved commercially through RT-PCR, where a sample of the RNA transcript is isolated through a nasopharyngeal swab and reverse transcribed followed by which the sample undergoes PCR for quantification and determination of a positive or negative COVID-19 result. This method is expensive, taking place at commercial labs predominantly and somewhat time intensive. As such, our lab developed a 35–55-minute approach for the direct detection of SARS-CoV-2.[36] Rapid detection has the potential to reduce spread of the disease. We have also previously shown viral RNA detection for Zika and Dengue viruses,

also plaguing our communities.[36] Biomarkers are important and furthermore, the study of nucleic acid biomarkers like these and lncRNAs are integral to developing a deeper and more comprehensive understanding of the genetic mechanisms of the human body and how we treat certain diseases.

Materials and Methods

Linearization of M13 DNA

We obtained circular M13mp18 single-stranded DNA (New England Biolabs, cat. no. N4040S) and verified the concentration using the Nanodrop. Following this, we prepared 100 µl batches of linearized M13 by mixing 20 µl of circular M13 DNA, 10 µl of 10x cutsmart buffer (New England Biolabs, cat. no. B7204S; included with BtsCI enzyme purchase), 4 µl of cutsite oligo (Integrated DNA Technologies, IDT) and 66 µl of nuclease free water (ultrapure distilled water, DNase, and RNase free, Invitrogen, cat. no. 10977-015). BtsCI enzyme can only cleave double-stranded DNA, as a result of this, the cutsite oligo was needed to make the M13 DNA double stranded so the cleavage was possible.

This mixture was collected into a PCR tube and annealed in a thermocycler by heating to 95 ºC and cooling to 50 ºC. At this temperature, 4 µl of BtsC1 restriction enzyme (20,000 U/ml; New England Biolabs, cat. no. R0647S) was added. We pipetted the mixture thoroughly using a 100 µl pipette. The annealing protocol was resumed, and the mixture was incubated at 50 ºC for 15 minutes. After the additional incubation period, the sample was reheated to 90 ºC (to denature the enzyme) and cooled to 4 ºC. The 100 µl mixture of linearized M13 was then stored in a -20 ºC freezer.[35]

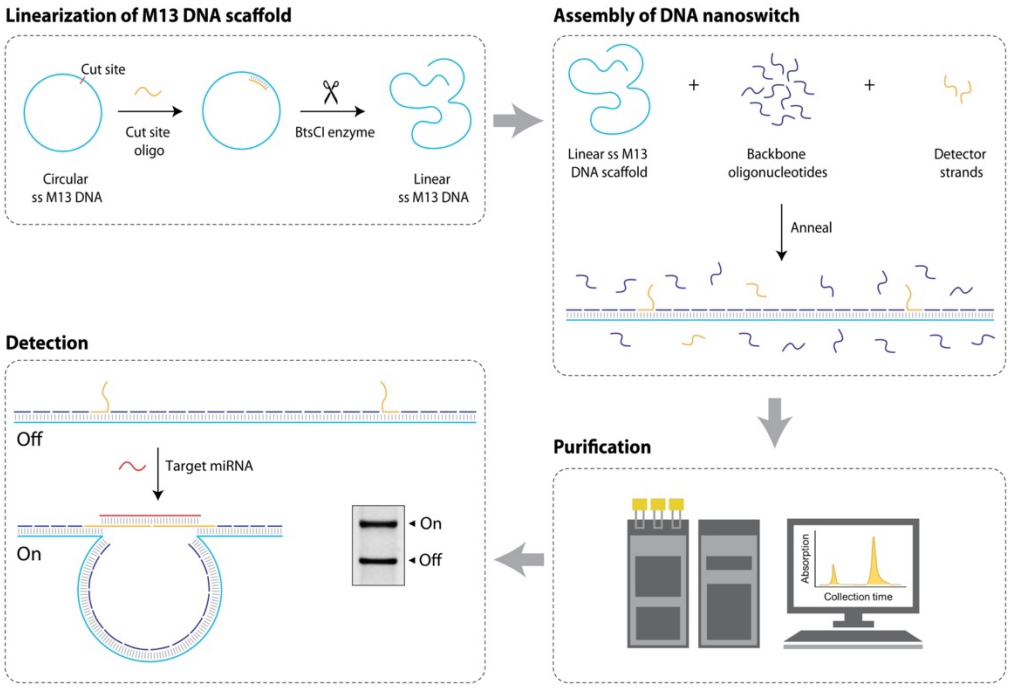

Figure 2. DNA nanoswitch construction, purification, and detection

The DNA nanoswitch is constructed from a BtsCI linearized ssDNA M13 scaffold which has been annealed with backbone oligonucleotides and detector strands specific to a target. These nanoswitches are purified using high performance liquid chromatography to remove excess oligonucleotides. The nanoswitch is validated upon incubation with the target where it undergoes a conformational change that is visualized and analyzed through agarose gel electrophoresis. Reproduced from ref.[38]

DNA nanoswitch construction

The DNA nanoswitch was formed by annealing the linearized M13 DNA to a mixture of backbone oligonucleotides and detector strands following protocols previously established in the lab (Figure 2).[38] Linearized M13 was mixed with 10x molar excess of complementary backbone oligonucleotides and detector strands. The mixture was then annealed using a temperature ramp from 90 ºC to 25 ºC at 1 ºC/min. Annealed DNA nanoswitches were purified from excess

oligonucleotides using high performance liquid chromatography (HPLC) with methods we previously established.[42]

Preparation of in vitro transcribed (IVT) RNA

As an experimental control for long RNAs, we prepared a 1260 nt RNA by in-vitro transcription using RNA Clean & Concentrator-25 kit (Zymo Research, Cat# R1017). The control template was mixed with T7 polymerase mix, 900 µg/ml of PVSA (Polyvinyl sulfonic acid), NTP Buffer mix and nuclease free water. The mixture was transcribed at 37 ºC for 2 hours following which it was treated with DNase I (2000U/ml). Incubation at 37 ºC was resumed for an additional 15 minutes. The IVT RNA was precipitated by incubation with LiCl at -80 ºC for 60 minutes. Following this, the sample was transferred to a 1.5 ml tube and centrifuged (10,000 g) for 15 minutes to pellet the IVT RNA. The supernatant (LiCl and other contaminants) was removed, and the pellet was washed with 500 ml of iced 70% ethanol. The sample was centrifuged (10,000 g) for 5 minutes and the ethanol was removed. The pellet was left to dry following which the sample was resuspended in 100 µl of nuclease free water. The concentration was determined using the Nanodrop spectrophotometer. IVT RNA was stored at -80 ºC.

DNA nanoswitch assay

DNA nanoswitches were validated by incubating them with synthetic target DNA. 100 µM stock concentration of the DNA was made per manufacturer's sheet. Following this, the actual concentration was ascertained using a Nanodrop spectrophotometer and then dilutions of the target DNA were made at 1 µM and 25 nM. DNA nanoswitches were tested using the 25 nM target to determine whether they worked by mixing 1x final of PBS, 10 mM $MgCl_2$, nuclease free water, DNA nanoswitches and synthetic target DNA in a 10 µl reaction. Negative controls were done by

replacing the DNA target with nuclease free water. All samples were incubated for a minimum of 30 minutes at various incubation temperatures, then mixed with Gel Red and loading dye, and run on a 0.8% agarose gel for 45 minutes at 75 V.

Agarose gel electrophoresis

0.8% agarose gels in 0.5x TBE buffer (Tris Boric EDTA) were made. Unless otherwise specified, samples of nanoswitches with targets and their respective controls were mixed with Gel Red and 6x loading dye (Ficoll based loading dye with Bromophenol blue) to a final 1X concentration. 10µl of this reaction mixture was loaded into each well. Gels were typically run at 75V for 45 minutes at room temperature. All gels were imaged using Image Lab software and the bands are quantified.

RNA Fragmentation

We fragmented the invitro transcribed long RNA using 5xTris HCl fragmentation buffer consisted of 15 mM $MgCl_2$ and 100 mM Tris-HCl at a pH of 8.5. We carried out fragmentation by mixing long RNA with the fragmentation buffer (at a final of 1x) and nuclease-free water. Following the set-up of the reaction mixture, we heated the samples at 94 ºC for various time points from 0 minutes to 64 minutes to fragment the RNA.

Detection of fragmented long RNA

We designed DNA nanoswitches to target a specific region of the long RNA. The long RNA was mixed with either buffer (1x final) in a 5 µl reaction for fragmentation. Samples were fragmented at 94 ºC for 0, 2, 4, 8, 16, 32, and 64 minutes. Following fragmentation, 1 µl of the fragmented

samples were mixed with 1 µl of HPLC purified DNA nanoswitches, 2 µl of a 5x incubation buffer and 6 µl of nuclease free water. The 5x incubation buffer was created as a standard mix of 1 µl of 5% SDS, 3 µl of 1 M $MgCl_2$, 2 µl of 100 µM blocking oligo and 13 µl of nuclease free water. All samples were incubated for 110 minutes at 50 ºC in a thermocycler. 5 µl of 100 mM EDTA was added, and incubation resumed for an additional 10 minutes. All samples were then treated with 1:2 loading mixture (1:1000 dilution of Gel Red and 6x loading dye diluted in 5 µl of nuclease free water). 8 µl of the sample was run on a 0.8% agarose gel.

Detection in the presence of total RNA

We spiked in the in vitro transcribed Long RNA into murine skeletal muscle total RNA (Biochain, cat. no. R1334171-50). The long RNA was fragmented in 5x Tris-HCl and 1 µl of the fragmented RNA (1 ng/µl) was added to the total RNA to test detection. Negative and positive controls were done in buffer (final reaction concentration of 1x PBS and 10mM $MgCl_2$ (no total RNA) with the negative control having no DNA target and the positive control having the DNA target. The DNA nanoswitch detection assay was then performed on the buffer controls as well as the spiked in samples of the total RNA.

Results and Discussion

As a first step towards the detection of long non-coding RNAs, we made long RNA using in vitro transcription. In vitro transcription was done so we would have a template for assay optimization tests as long non-coding RNAs are precious. We tested the concentration of the in vitro transcribed long RNA using a Nanodrop spectrophotometer to ensure it was suitable for optimization tests. Some of the concentrations obtained from various transcriptions were 41.2 ng/µl, 131.8 ng/µl, 120.5 ng/µl, and 136.7 ng/µl. An aliquot of each of these samples was taken to achieve a pooled sample concentration of 109 ng/µl. To validate proper in vitro transcription, we tested one of the samples on a 0.8% agarose gel along with a single stranded RNA (ssRNA) ladder (Figure 3). The migration of the long RNA band matched the expected length of the transcribed RNA (1260 nt), migrating between the 1000 nt and 2000 nt bands of the ssRNA ladder. This indicated a proper IVT reaction. Since the sample of long RNA was run on a native, nondenaturing agarose gel, the upward smear bands are indicative of possible secondary structures of the long RNA.

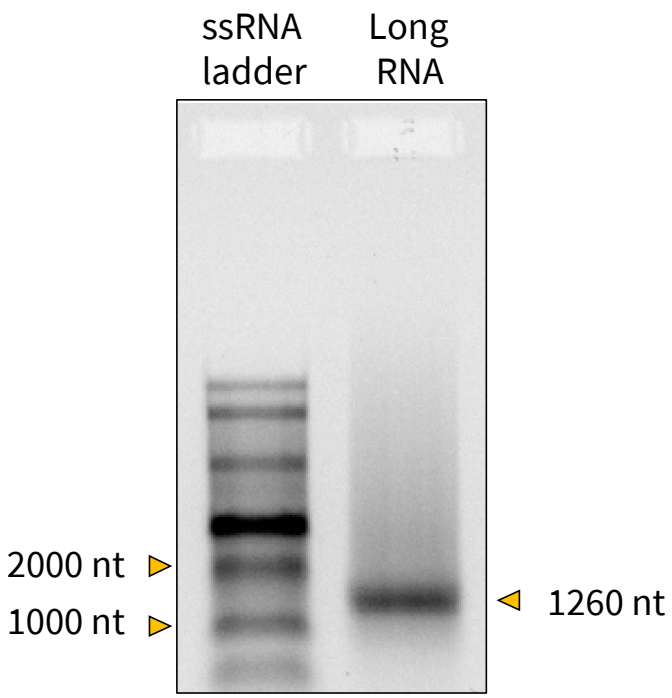

Figure 3. Characterization of long RNA

The long RNA was run on a 0.8% agarose gel. The band corresponding to the long RNA migrated at the range between the 1000 and 2000 nt bands of a ssRNA ladder, indicating proper IVT of the 1260 nt RNA.

To test detection of the target RNA, we first constructed nanoswitches that were specific to a 60 nt region of the long RNA. We validated the nanoswitches by incubating them with a 60 nt synthetic DNA target, analogous to the targeted sequence of the long RNA (Figure 4a). We incubated the nanoswitches with 25 nM of the synthetic DNA target and confirmed working of the nanoswitches on an agarose gel (Figure 4b). The presence of the "on" band in the gel indicated that the nanoswitch detectors bound the target and reconfigured into the looped state.

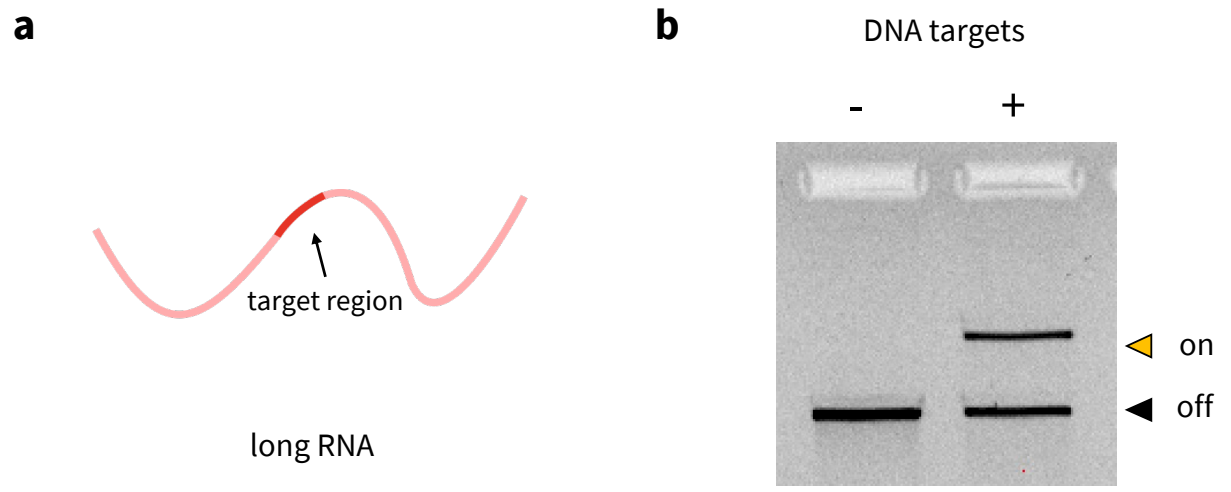

Figure 4. Depiction of long RNA and run of DNA target with DNA nanoswitch

(a) Depiction of long RNA (pink) with the target region in red. (b) Agarose gel showing reconfiguration of the nanoswitch in the presence of target DNA. The (+) and (-) indicate presence or absence of the target.

In previous work on detecting viral RNAs, the target RNA (~11,000 nt) was fragmented to achieve detection using DNA nanoswitches. Based on those results, we fragmented the long RNA by heating it at 94 ºC in 5xTris HCl buffer for different time points. Results showed that the size of the fragments decreased with increasing fragmentation time as seen by lowered-mobility bands on the gel during the time course (Figure 5). As heat fragmentation is random, the target region may be randomly cleaved and even fully degraded decreasing their detection potential. As such, we designed and constructed nanoswitches with variable detector lengths to address this (Figure 6a). To test the nanoswitches, we incubated them with a 60 nt DNA target at 20 ºC and at 50 ºC for 1 hour. Results showed that samples incubated at 50 ºC yielded higher detection signals than the samples incubated at 20 ºC as the bands were more visible on the gel after imaging (Figure 6b). These results indicated that the higher incubation temperature was well-suited to the base pairing

of the DNA target sequence with the detectors of the DNA nanoswitches. Further, the variability in detection among DNA nanoswitches of variable detector lengths may be attributed to complete base pairing versus incomplete base pairing of sequences.

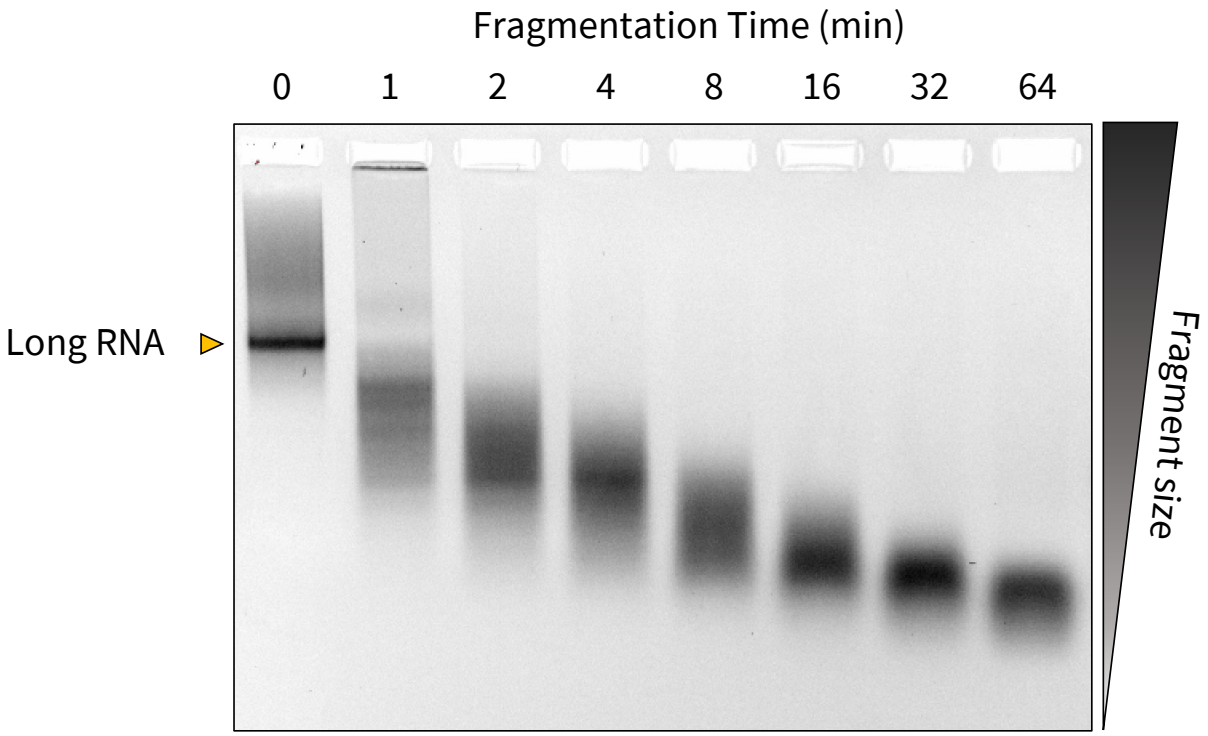

Figure 5. Fragmentation of long RNA at increasing fragmentation time points

As shown by the triangular grey bar on the side, the size of the fragments decreases with increasing fragmentation time.

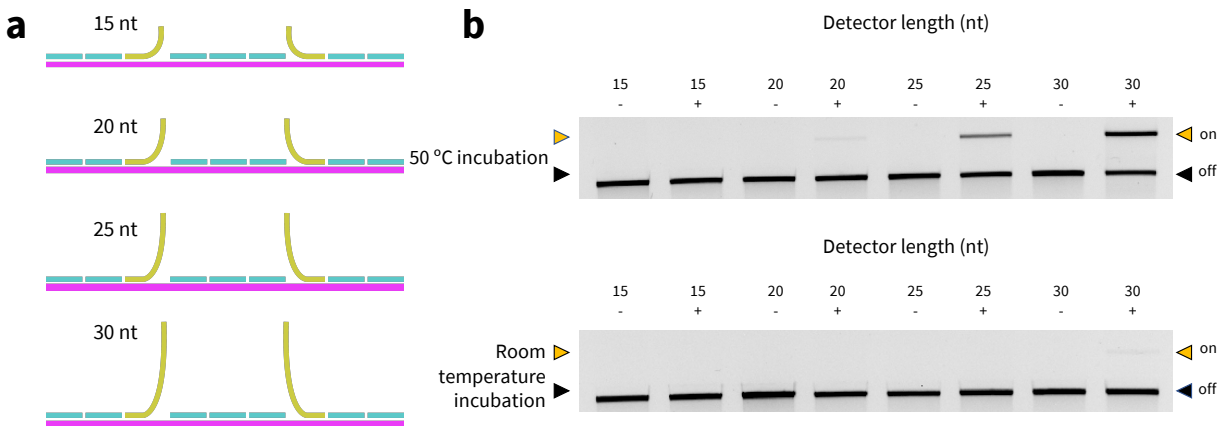

Figure 6. Detector length illustration and incubation temperature tests

(a) Illustration showing nanoswitches with 15 nt to 30 nt long detectors. The 15 nt nanoswitches can bind to a total of 30 nts of the target sequence while the 20 nt detectors would bind a total of 40 nts of the target sequence and so forth. Color code (green = detector strands, pink = M13 scaffold, blue = backbone oligonucleotides). (b) Nanoswitches with different detector lengths incubated with DNA targets at 50 ºC (top gel) and room temperature (bottom gel) for 1 hour. Detection signal increased for 20, 25 and 30 nt detectors under 50 ºC incubation. Visible detection was achieved for 30 nt detector nanoswitches at room temperature.

Next, we fragmented our long RNA using a 5x Tris HCl fragmentation buffer made in-house (the buffer is a mixture of 15 mM $MgCl_2$ and 100 mM Tris-HCl at a final pH of 8.5). We set up fragmentation with the long RNA and Tris HCl fragmentation buffer (1x final). Following long RNA fragmentation, we incubated the DNA nanoswitches with the fragmented long RNA at 50 ºC for a total of 2 hours. The results obtained showed no visible detection of the fragmented long RNA with the 15 nt detector DNA nanoswitches (Figure 7). The 20 nt detector nanoswitches showed visible detection with long RNAs fragmented for 2 to 16 minutes. The brightest detection signals were determined to be from long RNA fragmented for 8 and 16 minutes with the 30 nt detector nanoswitches (indicated by the red box in Figure 7).

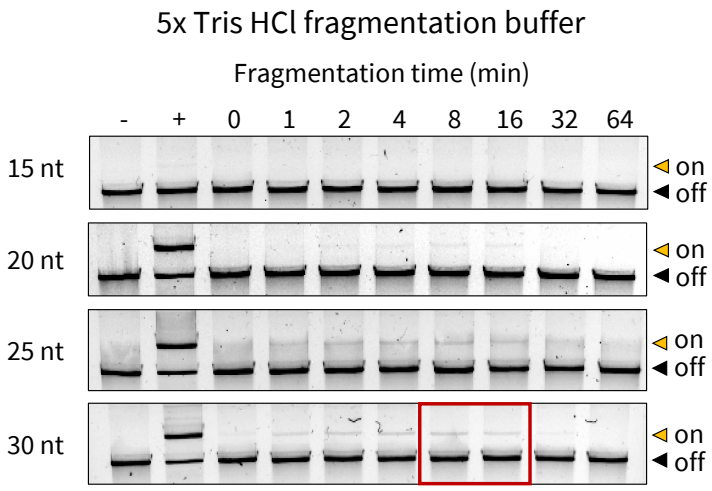

Figure 7. Detector length and 5x Tris HCl fragmentation time course

The bands were quantified in image lab and the results showed the brightest and most uniform bands at 8- and 16-minute fragmentation (boxed in red).

Next, we determined the detection limit of our 30 nt detector DNA nanoswitches by testing detection of different concentrations of long RNA fragmented with 5xTris HCl buffer. We incubated the 30 nt detector DNA nanoswitches with increasing amounts of long RNA fragmented at 8 minutes. The incubation conditions were set to 50 ºC for 1 hour and 50 minutes followed by the addition of 5µl of 100 mM EDTA. The samples were incubated for an additional 10 minutes. After imaging, we determined visible detection at 18.8 pM or 62.5 pg of fragmented RNA (Figure 8a and 8b).

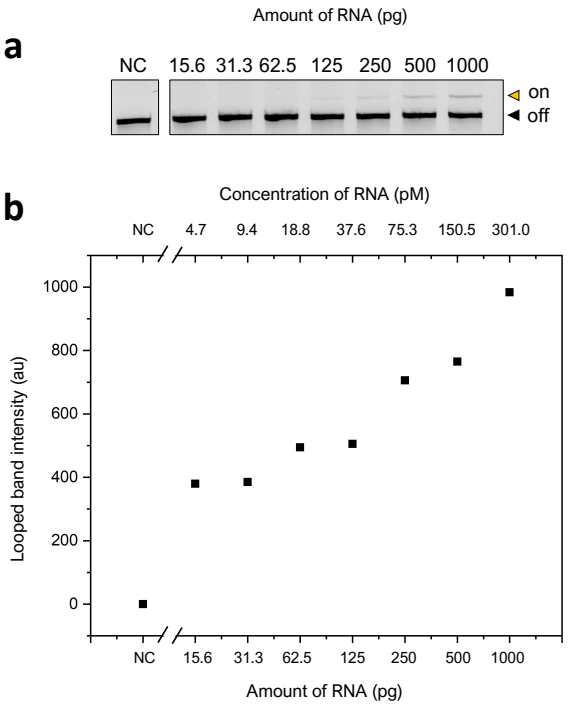

Figure 8. Concentration series detection of long RNA

(a) Gel image showing detection of different amounts of long RNA. Visible detection was achieved at 62.5 pg. (NC = negative control where no RNA is present). (b) Graph showing the quantification of the "on" bands in (a) (au = arbitrary units).

We further tested the ability of our nanoswitches to detect the fragmented long RNA in the presence of total RNA (Figure 9). We did tested detection in the presence of unfragmented total RNA by incubating the DNA nanoswitches in buffer with and without a target DNA sequence (positive and negative controls, respectively) to ensure the nanoswitches were functional. Then we set up three samples for incubation of DNA nanoswitches with 500 ng/µl total RNA obtained from murine skeletal muscle cells: (1) 25nM of the DNA target spiked into the total RNA as an additional control to determine the location of the looped band on the gel in the presence of unfragmented total RNA, (2) the nanoswitch only in the total RNA, and (3) 1 ng/µl fragmented

long RNA spiked into the unfragmented total RNA. Our results showed that the nanoswitch was able to detect the fragmented RNA in the presence of unfragmented total RNA (Figure 9, lane 5). Further, this detection was specific to detect the target RNA in a biological sample mimic as there was no unspecific binding or false positive results (shown in total RNA and nanoswitch only gel lane, Figure 9, lane 4). As future steps, nanoswitches specific to known lncRNAs are being designed and will be tested by fragmenting total RNA to increase the detection signal in accordance with our current assay and limit the formation of complex secondary structures. The fragmented total RNA will be incubated with DNA nanoswitches to test detection.

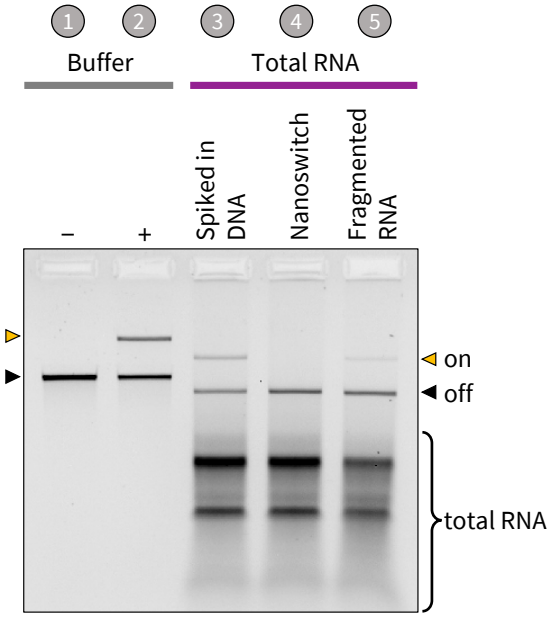

Figure 9. Detection in the presence of total RNA

From left to right: (1) Negative control in buffer, (2) positive control in buffer, (3) DNA target spike-in in the presence of total RNA, (4) DNA nanoswitch only in total RNA, (5) fragmented RNA spiked into total RNA. The "on" band indicating detection is shown by the yellow arrow on the right. The shift of the bands in lanes 3-5 is due to the additional RNA present in total RNA causing additional drag of the DNA nanoswitches through the gel.

Conclusion

DNA nanoswitches are biosensing devices that can be utilized for the detection of nucleic acids including miRNAs and viral RNAs. Here, we report a simple, low-cost strategy for the detection of long RNAs in a bench-top laboratory setting as a blueprint towards the detection of lncRNAs. Our strategy utilizes heat fragmentation (1x Tris HCl buffer at 94 ºC) to fragment long RNAs which increases the detection signal of our assay. Due to the random nature of fragmentation, we utilized the programmable nature of our DNA nanoswitches to create nanoswitches with variable detector lengths ranging from 15 nt to 30 nt. The results of our assay showed that 30 nt detector nanoswitches yielded the brightest detection signals for the detection of 8- and 16-minute fragmented long RNAs at 50 ºC incubation.

Further, we have shown that our nanoswitches are sensitive to low concentrations of fragmented long RNA where we achieved visible detection of 62.5 pg of fragmented long RNA. We also showed that our nanoswitches were target specific when we tested our assay in the presence of total RNA. As we go towards the detection of lncRNAs, our next steps include designing DNA nanoswitches specific to known lncRNAs and then testing for detection in cell- or tissue-specific total RNA. Following initial detection of lncRNAs present in total RNA would be optimization tests to increase detection signals. Our nanoswitch assay has the potential to add to the existing strategies for lncRNA detection, providing an efficient and affordable alternative for the detection of lncRNAs as potential biomarkers for various conditions and diseases.

References

1. Amur, S. Biomaker terminology: Speaking the same language. https://www.fda.gov/files/BIOMARKER-TERMINOLOGY--SPEAKING-THE-SAME-LANGUAGE.pdf
2. Haskell, R. What is a biomarker? https://www.nursingcenter.com/ncblog/november-2019/biomarker (2019).
3. Hanash, S. M., Baik, C. S. & Kallioniemi, O. Emerging molecular biomarkers—blood-based strategies to detect and monitor cancer. *Nat. Rev. Clin. Oncol.* **8**, 142–150 (2011).
4. Ponting, C. P., Oliver, P. L. & Reik, W. Evolution and Functions of Long Noncoding RNAs. *Cell* **136**, 629–641 (2009).
5. Mercer, T. R., Dinger, M. E. & Mattick, J. S. Long non-coding RNAs: Insights into functions. *Nat. Rev. Genet.* **10**, 155–159 (2009).
6. Statello, L., Guo, C.-J., Chen, L.-L. & Huarte, M. Gene regulation by long non-coding RNAs and its biological functions. *Nat. Rev. Mol. Cell Biol.* **22**, 96–118 (2021).
7. Lee, J. T. Epigenetic Regulation by Long Noncoding RNAs. *Science* **338**, 1435–1439 (2012).
8. Yao, R.-W., Wang, Y. & Chen, L.-L. Cellular functions of long noncoding RNAs. *Nat. Cell Biol.* **21**, 542–551 (2019).
9. Schmitt, A. M. & Chang, H. Y. Long Noncoding RNAs in Cancer Pathways. *Cancer Cell* **29**, 452–463 (2016).
10. Liu, S. J., Dang, H. X., Lim, D. A., Feng, F. Y. & Maher, C. A. Long noncoding RNAs in cancer metastasis. *Nat. Rev. Cancer* **21**, 446–460 (2021).
11. Marques, F. Z., Booth, S. A. & Charchar, F. J. The emerging role of non-coding RNA in essential hypertension and blood pressure regulation. *J. Hum. Hypertens.* **29**, 459–467 (2015).

12. Dechamethakun, S. & Muramatsu, M. Long noncoding RNA variations in cardiometabolic diseases. *J. Hum. Genet.* **62**, 97–104 (2017).

13. Bao, M.-H. et al. Long non-coding RNAs in ischemic stroke. *Cell Death Dis.* **9**, 281 (2018).

14. Wapinski, O. & Chang, H. Y. Long noncoding RNAs and human disease. *Trends Cell Biol.* **21**, 354–361 (2011).

15. Mouraviev, V. et al. Clinical prospects of long noncoding RNAs as novel biomarkers and therapeutic targets in prostate cancer. *Prostate Cancer Prostatic Dis.* **19**, 14–20 (2016).

16. Liu, D., Mewalal, R., Hu, R., Tuskan, G. A. & Yang, X. New technologies accelerate the exploration of non-coding RNAs in horticultural plants. *Hortic. Res.* **4**, 17031 (2017).

17. Liu, S. J. et al. Single-cell analysis of long non-coding RNAs in the developing human neocortex. *Genome Biol.* **17**, 67 (2016).

18. Sun, Q., Hao, Q. & Prasanth, K. V. Nuclear long noncoding RNAs: Key regulators of gene expression. *Trends Genet.* **34**, 142–157 (2018).

19. Uchida, S. High-throughput methods to detect long non-coding RNAs. *High-Throughput* **6**, 12 (2017).

20. Xiao, M. et al. Rationally engineered nucleic acid architectures for biosensing applications. *Chem. Rev.* **119**, 11631–11717 (2019).

21. Chandrasekaran, A. R. *et al.* DNA nanotechnology approaches for microRNA detection and diagnosis. *Nucleic Acids Res.* **47**, 10489–10505 (2019).

22. Xavier, P. L. & Chandrasekaran, A. R. DNA-based construction at the nanoscale: Emerging trends and applications. *Nanotechnology* **29**, 062001 (2018).

23. Chandrasekaran, A. R., Anderson, N., Kizer, M., Halvorsen, K. & Wang, X. Beyond the fold: Emerging biological applications of DNA origami. *ChemBioChem* **17**, 1081–1089 (2016).

24. Seeman, N. C. & Sleiman, H. F. DNA nanotechnology. *Nat. Rev. Mater.* **3**, 17068 (2018).

25. Madhanagopal, B. R., Zhang, S., Demirel, E., Wady, H. & Chandrasekaran, A. R. DNA nanocarriers: Programmed to deliver. *Trends Biochem. Sci.* **43**, 997–1013 (2018).

26. Gangrade, A., Stephanopoulos, N. & Bhatia, D. Programmable, self-assembled DNA nanodevices for cellular programming and tissue engineering. *Nanoscale* **13**, 16834–16846 (2021).

27. Rangnekar, A. & LaBean, T. H. Building DNA Nanostructures for molecular computation, templated assembly, and biological applications. *Acc. Chem. Res.* **47**, 1778–1788 (2014).

28. Zhirnov, V., Zadegan, R. M., Sandhu, G. S., Church, G. M. & Hughes, W. L. Nucleic acid memory. *Nat. Mater.* **15**, 366–370 (2016).

29. Dai, M. 3D DNA nanostructure. (Springer New York, 2017)

30. Surana, S., Bhat, J. M., Koushika, S. P. & Krishnan, Y. An autonomous DNA nanomachine maps spatiotemporal pH changes in a multicellular living organism. *Nat. Commun.* **2**, 340 (2011).

31. Pei, H. *et al.* A DNA Nanostructure-based biomolecular probe carrier platform for electrochemical biosensing. *Adv. Mater.* **22**, 4754–4758 (2010).

32. Pfeiffer, M. et al. Single antibody detection in a DNA origami nanoantenna. *iScience* **24**, 103072 (2021).

33. Koussa, M. A., Halvorsen, K., Ward, A. & Wong, W. P. DNA nanoswitches: a quantitative platform for gel-based biomolecular interaction analysis. *Nat. Methods* **12**, 123–126 (2015).

34. Chandrasekaran, A. R., Zavala, J. & Halvorsen, K. Programmable DNA nanoswitches for detection of nucleic acid sequences. *ACS Sens.* **1**, 120–123 (2016).

35. Chandrasekaran, A. R., Dey, B. K. & Halvorsen, K. How to perform miRacles: A step-by-step microRNA detection protocol using DNA nanoswitches. *Curr. Protoc. Mol. Biol.* **130**, (2020).

36. Zhou, L. et al. Programmable low-cost DNA-based platform for viral RNA detection. *Sci. Adv.* **6**, eabc6246 (2020).

37. Chandrasekaran, A. R. & Halvorsen, K. DNA-based smart reagent for detecting Alzheimer's associated microRNAs. *ACS Sens.* **6**, 3176–3181 (2021).

38. Chandrasekaran, A. R. et al. Cellular microRNA detection with miRacles: MicroRNA-activated conditional looping of engineered switches. *Sci. Adv.* **5**, eaau9443 (2019).

39. Chandrasekaran, A. R. et al. DNA Nanoswitch barcodes for multiplexed biomarker profiling. *Nano Lett.* **21**, 469–475 (2021).

40. Chandrasekaran, A. R., Trivedi, R. & Halvorsen, K. Ribonuclease-responsive DNA Nanoswitches. *Cell Rep. Phys. Sci.* **1**, 100117 (2020).

41. Ebert, M. S. & Sharp, P. A. Roles for microRNAs in conferring robustness to biological processes. *Cell* **149**, 515–524 (2012).

42. Halvorsen, K., Kizer, M. E., Wang, X., Chandrasekaran, A. R. & Basanta-Sanchez, M. Shear dependent LC purification of an engineered DNA nanoswitch and implications for DNA origami. *Anal. Chem.* **89**, 5673–5677 (2017).